

Biomedical Materials



PAPER

Preparation and characterization of a decellularized cartilage scaffold for ear cartilage reconstruction

RECEIVED
9 September 2014

REVISED
26 October 2014

ACCEPTED FOR PUBLICATION
4 December 2014

PUBLISHED
13 January 2015

Lizette Utomo^{1,2,3,9}, Mieke M Pleumeekers^{1,9}, Luc Nimeskern⁴, Sylvia Nürnberger^{5,6,7}, Kathryn S Stok⁴, Florian Hildner^{6,8} and Gerjo J V M van Osch^{1,2}

¹ Department of Otorhinolaryngology, Erasmus MC, University Medical Center Rotterdam, Wytemaweg 80, 3015 CN, Rotterdam, The Netherlands

² Department of Orthopaedics, Erasmus MC, University Medical Center Rotterdam, Wytemaweg 80, 3015 CN, Rotterdam, The Netherlands

³ Faculty of Science and Technology, University of Twente, PO Box 217, 7500 AE Enschede, The Netherlands

⁴ Institute for Biomechanics, ETH Zürich, Wolfgang-Pauli-Strasse 10, 8093 Zürich, Switzerland

⁵ Department of Traumatology, Medical University of Vienna, Währinger Gürtel 18–20, 1090 Vienna, Austria


⁶ Ludwig Boltzmann Institute for Experimental and Clinical Traumatology, AUVA Research Center, Austrian Cluster for Tissue Regeneration, Donauschlingenstrasse 13, 1200 Vienna, Austria

⁷ Bernhard Gottlieb University Clinic of Dentistry, Sensengasse 2a, A-1090 Vienna, Austria

⁸ Red Cross Blood Transfusion Service of Upper Austria, Krankenhausstraße 7, 4017 Linz, Austria

E-mail: g.vanosch@erasmusmc.nl

Keywords: decellularization, cartilage, scaffold, ear reconstruction, mechanical properties

 Online supplementary data available from stacks.iop.org/BMM/10/015010

Abstract

Scaffolds are widely used to reconstruct cartilage. Yet, the fabrication of a scaffold with a highly organized microenvironment that closely resembles native cartilage remains a major challenge. Scaffolds derived from acellular extracellular matrices are able to provide such a microenvironment. Currently, no report specifically on decellularization of full thickness ear cartilage has been published. In this study, decellularized ear cartilage scaffolds were prepared and extensively characterized. Cartilage decellularization was optimized to remove cells and cell remnants from elastic cartilage. Following removal of nuclear material, the obtained scaffolds retained their native collagen and elastin contents as well as their architecture and shape. High magnification scanning electron microscopy showed no obvious difference in matrix density after decellularization. However, glycosaminoglycan content was significantly reduced, resulting in a loss of viscoelastic properties. Additionally, in contact with the scaffolds, human bone-marrow-derived mesenchymal stem cells remained viable and are able to differentiate toward the chondrogenic lineage when cultured *in vitro*. These results, including the ability to decellularize whole human ears, highlight the clinical potential of decellularization as an improved cartilage reconstruction strategy.

1. Introduction

Ear cartilage defects—either caused by congenital malformation, trauma or tumor destruction—are a commonly encountered problem in reconstructive surgery, since cartilage has a limited capacity for self-regeneration once damaged. Therefore, ear cartilage defects can ultimately lead to physical and aesthetic impairment. Despite the great demand for treating ear cartilage defects, current treatments using autologous

cartilage are challenging. Not only because they require a high degree of surgical expertise, but also because they are associated with limited availability of autologous cartilage and can cause severe donor site morbidity.

For successful cartilage reconstruction, the properties of the three-dimensional (3D) matrix is of major importance, in: (1) providing temporary or permanent support while maintaining size and shape; and (2) providing specific structural, mechanical and biological cues to cells, which guide tissue remodeling [1, 2]. Ideally, the best scaffold for cartilage reconstruction should mimic the extracellular matrix (ECM) of the targeted tissue itself. As a result, several 3D scaffolds,

⁹ Both authors contributed equally.

including both natural and synthetic materials, have been developed and investigated for their use in cartilage reconstruction [3–5]. A frequently used alternative to autologous cartilage implants are synthetic materials such as porous polyethylene [6,7]. Although this material is advantageous to work with it is prone to induce a foreign body reaction, the ensuing extrusion [8] in most cases resulting in removal of the entire implant [9]. Additionally, the biomechanical mismatch of the implants compared to normal ear cartilage can result in eventual collapse of the framework [10]. So far, no ideal scaffold has emerged since the complex 3D composition and architecture of native ECM makes it extremely difficult to precisely mimic. Recently, natural acellular ECM scaffolds have become increasingly popular. These acellular ECM scaffolds are acquired by a process called decellularization: a method that requires chemical, physical and/or enzymatic treatments [11]. Decellularized ECM scaffolds provide a 3D ECM structure with immediate functional support without evoking an adaptive immune response upon implantation due to absence of donor cellular antigens [12].

To date, various cartilaginous structures have already been decellularized including tracheal cartilage [12–17], articular cartilage [18–21], nasal cartilage [22, 23], intervertebral discs [24, 25] and meniscal cartilage [22, 26–28]. Currently, no method to specifically decellularize full thickness ear cartilage that belongs to the elastic cartilage type, has been described in literature. In contrast to hyaline and fibrous cartilage, elastic cartilage contains additional thick elastic fibers, making it denser and therefore more challenging to decellularize. Furthermore, the ability to prepare scaffolds from whole cartilage tissue rather than scaffolds that are derived from ECM [29, 30], provides the opportunity to decellularize large tissues and structures that hold complex native shapes such as ears.

Therefore, the goal of this study was to prepare decellularized ear cartilage scaffolds and extensively characterize their biochemical and biomechanical properties, as well as investigate their cytocompatibility. Furthermore, by preparing human ear cartilage scaffolds with desirable size and shape, we show the potential of decellularized cartilage to improve human cartilage reconstruction.

2. Materials and methods

All chemicals were obtained from Sigma-Aldrich, St. Louis, USA unless stated otherwise.

2.1. Preparation of decellularized cartilage scaffolds

To obtain full thickness bovine ear cartilage (bEC), macroscopically intact cartilage was harvested from calves ($n = 3$) less than 8 months old (T. Boer & Zn., Nieuwerkerk aan den IJssel, the Netherlands) and washed with phosphate buffered saline (PBS) after careful resection of the perichondrium. Bovine

articular cartilage samples (bAC) were harvested from the metacarpophalangeal joints ($n = 3$) and included as controls to compare decellularization outcomes. Samples were made using an 8 mm dermal biopsy punch (Spengler, Asnières sur Seine, France) and kept in PBS until decellularization. Human ear cartilage (hEC) was obtained from post mortem donors ($n = 2$; M, 83 and 84 Y) who donated their bodies to medical science at Erasmus Medical Center (EMC; Rotterdam, the Netherlands). Dermal tissue was macroscopically removed, followed by careful removal of the perichondrium and samples were made using an 8 mm dermal biopsy punch. Untreated (i.e. native) cartilage samples were immediately stored dry at -80°C after harvest for biochemical analysis or in 4% formaldehyde for histological analysis and scanning electron microscopy (SEM).

All human and bovine cartilage samples were decellularized according to the protocol of Kheir *et al* [19], which was further optimized to specifically decellularize ear cartilage. Briefly, the samples were subjected to two overnight dry freeze-thaw cycles followed by two overnight freeze-thaw cycles at -20°C in hypotonic buffer (10mM tris-HCl in Mili-Q water, pH 8.0) following a 24 h incubation in hypotonic buffer at 45°C . Next, samples were treated for 24 h with an ionic detergent consistent of 0.1% sodium dodecyl sulfate (SDS), 0.1% ethylenediaminetetraacetic acid (EDTA) and 10 KIU ml^{-1} aprotinin in Mili-Q water. Then, samples were washed twice for 30 min in wash solution (PBS with 10 KIU ml^{-1} aprotinin) before a 24 h wash at 45°C in wash solution. Since the protocol of Kheir *et al* was not sufficient to reduce or remove cellular remnants, an elastase solution was incorporated into the protocol to improve the removal of cellular remnants. Therefore, the samples were treated next with a low concentration elastase solution (0.2M tris-HCl in Mili-Q water, 10 KIU ml^{-1} aprotinin and 0.03 U ml^{-1} elastase, pH 8.6) for 24 h at 37°C , as a high concentration elastase would completely damage the matrix structure due to the complete depletion of elastin and glycosaminoglycans (GAGs). (Online supplementary figure 1 (stacks.iop.org/BMM/10/015010).) Next, samples were washed twice and incubated for 3 h at 37°C in nuclease solution (50mM tris-HCl in Mili-Q water, 10mM MgCl, 50 $\mu\text{g ml}^{-1}$ bovine serum albumin (BSA), 50 U ml^{-1} DNase and 2.5 U ml^{-1} RNase, pH 7.5). Samples were washed again in wash solution and treated for 3 h in decontamination solution (0.1% peracetic acid in PBS). All incubation and wash steps were performed with agitation. Finally, the samples were transferred to sterile tubes and washed twice for 30 min in sterile PBS before starting a 24 h wash cycle in sterile PBS at 45°C . To assess the decrease in wet weight after decellularization, samples from one donor of both cartilage types were weighted directly after harvest and subjected to an individual decellularization treatment taking into account volume ratios of the used solutions. After the individual treatment, wet weight was determined

again. Samples from the remaining donors were decellularized in batches. Samples intended for histological analysis and SEM were stored in 4% formaldehyde and samples for biochemical analysis were stored dry at -80°C . Samples intended for biomechanical analysis were shipped to Eidgenössische Technische Hochschule (ETH; Zurich, Switzerland) in PBS containing protease inhibitors (Roche, Basel, Switzerland) at 4°C . Decellularized bEC scaffolds intended for seeding ($n = 1$, in 6-fold) were pre-conditioned for at least 2 h in Minimally Essential Medium Alpha (MEM- α ; Gibco, Carlsbad, USA) containing 10% fetal calf serum (FCS; Lonza, Verviers, Belgium), $50\ \mu\text{g ml}^{-1}$ gentamicin (Gibco) and $1.5\ \mu\text{g ml}^{-1}$ amphotericin B (Fungizone; Gibco) and stored at 4°C until seeding.

2.2. Biochemical analysis

Prior to biochemical analysis, wet weight was determined for all cartilage samples. For DNA, GAG and collagen analysis, samples were digested overnight at 60°C in a papain solution ($0.2\text{M Na}_2\text{H}_2\text{PO}_4$, $0.01\text{M EDTA}\cdot 2\text{H}_2\text{O}$, $250\ \mu\text{g ml}^{-1}$ papain, 5mM L-cystein , pH 6.0). Bovine and human cartilage samples were digested in $400\ \mu\text{l}$ and $500\ \mu\text{l}$ papain solution, respectively.

To assess the removal of nuclear components, the DNA content of the cartilage scaffolds was measured with the CyQUANT® (Invitrogen) proliferation assay. This assay is able to detect low amounts of DNA and has a detection limit of 10 ng per measurement. In short, 250 IU heparin (LEO Pharma, Ballerup, Denmark) and $125\ \mu\text{g}$ RNase were added to the papain digests and incubated for 30 min at 37°C . Finally, $0.375\ \mu\text{l}$ CyQUANT GR dye was added to each papain digested sample and fluorescence was immediately measured (excitation/emission: 480/520 nm) on a SpectraMax Gemini micro plate reader (Molecular Devices, Sunnyvale, USA), using calf thymus DNA as a standard.

A 1,9-Dimethylmethylene Blue (DMMB; pH 3.0) assay [31] was performed to measure the sulfated GAG content of the cartilage scaffolds. The metachromatic reaction of DMMB was monitored using a VersaMax spectrophotometer at 530 and 590 nm. Shark chondroitin sulfate C was used as a standard.

A hydroxyproline assay [32] was performed to measure the total amount of collagen of the cartilage scaffolds. In short, the papain digests were hydrolyzed with equal volumes of 12 M HCl at 108°C for 20 h, dried (Savant SPD 121P SpeedVac; Thermo Scientific, Massachusetts, USA) and re-dissolved in 1.5 ml Milli-Q water. Hydroxyproline contents were measured using a colorimetric method (extinction 570 nm), with chloramine-T and dimethylaminobenzaldehyde as reagents. Hydroxyproline (Merck) was used as a standard to calculate the amount of collagen per sample.

Elastin content of the cartilage samples was measured using the Fastin™ Elastin Assay (Biocolor, Carrickfergus, UK) according to manufacturer's instructions. Briefly, cartilage samples were converted to water soluble α -elastin by 3 overnight heat extraction cycles

at 100°C in 0.25M oxalic acid before adding the kit's dye. Absorption was measured at 513 nm on a VersaMax plate reader. α -elastin from bovine neck ligament (provided by manufacturer) was used as a standard.

2.3. Histological analysis

Untreated and decellularized samples were fixed in 4% formaldehyde and embedded in 3% agarose, dehydrated in an ascending series of alcohol, then embedded in paraffin and sectioned at $6\ \mu\text{m}$. Sections were stained with Gill's haematoxylin and eosin (H&E, Merck), Safranin-O and resorcin fuchsin (RF, Klinipath, Duiven, the Netherlands). Additionally, collagen type II and elastin were immunohistochemically visualized. Antigen retrieval for the collagen type II antibody (II-II 6B3; DSHB, Iowa, USA) was achieved by incubating in 0.1% pronase in PBS for 30 min at 37°C . Antigen retrieval of elastin (BA-4) was carried out by incubation in 0.25% trypsin in PBS for 20 min at 37°C . 10% goat serum in PBS was used to block non-specific binding sites. Next, sections were stained for 1 h with primary antibodies against collagen type II (1:100) or elastin (1:1000). An enzyme-streptavidin conjugate (HK-321/325-UK; Biogenex, California, USA) in PBS/1% BSA at a dilution of 1:100 was used as label and visualized by Neu Fuchsin substrate (Chroma, Köngen, Germany).

Cell-seeded cartilage scaffolds were immediately embedded in Tissue-Tek OCT Compound (Sakura, Alphen aan den Rijn, the Netherlands) after harvest, sectioned at $6\ \mu\text{m}$, fixed in acetone and stained with H&E.

For SEM analysis, samples were dehydrated in a graded alcohol series, fractured by pulling at the distal end of the samples and dried with hexamethyldisilazane. Samples were then mounted on stubs, coated with palladium gold in a sputter coater (SC7620; Emitech/Quorum Technologies, Loughton, UK) and visually observed with a scanning electron microscope (JSM-6510; JEOL, Tokyo, Japan).

2.4. Biomechanical testing

Biomechanical properties of cartilage scaffolds were assessed using stress-relaxation-indentation as previously described [33]. In short, samples ($n = 3$ with 6 samples per donor) were placed in close-fitting stainless steel cylindrical wells of 5 mm in diameter, while immersed in PBS supplemented with antibiotic/antimycotic solution. Mechanical testing was performed with a materials testing machine (Zwick Z005, Ulm, Germany) equipped with a 10 N load cell, a built-in displacement control, and a cylindrical, plane ended, stainless steel indenter ($\text{Ø}0.35\ \text{mm}$). A preload of 3 mN was first applied on the sample to locate the sample surface and measure sample thickness, and held for 5 min. Five consecutive strain steps in 5% increments were applied up to a maximum strain of 25%. Samples were then left to relax for 20 min at each step. A custom MATLAB® script was used to convert the force-displacement data to stress-strain. Maximum stress (σ_{max}) equilibrium modulus (E_{eq}), relaxation time (τ) and relaxation half

time ($t_{1/2}$) were determined from the stress–strain plots to determine intrinsic, flow-independent, and flow-dependent mechanical properties [34].

2.5. Scaffold cytocompatibility

To assess toxicity and complete removal of the used chemicals during decellularization, the scaffolds were evaluated for their cytotoxicity with a methylthiazolyldiphenyltetrazolium bromide (MTT) assay. Bone-marrow derived mesenchymal stem cells (BMSCs) were isolated from bone marrow aspirates from patients undergoing total hip-replacement surgery (3 males, 67 ± 5 Y), with informed consent and approval of the Medical Ethics Committee (Albert Schweitzer Hospital 2011/7). Cells were cultured at a density of 2300 cells cm^{-2} at 37 °C and 5% CO_2 in MEM- α , containing 10% FCS, 50 $\mu\text{g}/\text{mL}$ gentamicin, 1.5 $\mu\text{g}/\text{mL}^{-1}$ Fungizone, 25 $\mu\text{g}/\text{mL}^{-1}$ L-ascorbic acid 2-phosphate and 1 ng/mL basic Fibroblast Growth Factor 2 (bFGF2; R&D Systems, Minneapolis, USA), from now on referred to as ‘MSC-expansion medium’. For toxicity tests, BMSCs were plated in a 24-well plate at a density of 40 000 cells cm^{-2} and after 3 d of culture a decellularized cartilage scaffold was added to each well. Wells containing only medium or only BMSCs were included as controls. After 4 d, the cells and scaffolds were washed with PBS. Next, 5 mg/mL^{-2} MTT-solution was added and incubated for 3 h protected from light at 37 °C and 5% CO_2 . Finally, the scaffolds were removed from the wells and the MTT-solution was replaced with 100% ethanol (Boom, Meppel, the Netherlands), transferred to a 96-well plate and absorbance was measured at 670 and 570 nm on a VersaMax (Molecular Devices, Sunnyvale, USA). Toxicity experiments were conducted twice with independent BMSC and cartilage donors, with 3 decellularized bovine samples per cartilage type.

To further assess the interaction of cells with the decellularized cartilage scaffolds, BMSCs were seeded on the scaffolds by rotation in a tube rotator at 20 rpm (VWR, Radnor, Pennsylvania, USA) in 1.6 mL cell suspension containing 2×10^6 BMSCs/scaffold for 4 h at 37 °C. After seeding, the scaffolds were transferred to a 12-well plate (BD Biosciences) coated with 3% agarose (Eurogentec, Liège, Belgium) to prevent attachment of BMSCs to the culture well and cultured in 2 mL high glucose (4.5 g/l^{-1}) Dulbecco’s Modified Eagle Medium (DMEM-HG; Gibco) containing 50 $\mu\text{g}/\text{mL}^{-1}$ gentamicin, 1.5 $\mu\text{g}/\text{mL}^{-1}$ Fungizone, Insulin-Transferrin-Selenium (ITS + 1, BD Biosciences, New Jersey, USA), 40 $\mu\text{g}/\text{mL}^{-1}$ L-proline, 1 mM sodium pyruvate (Gibco), 25 $\mu\text{g}/\text{mL}^{-1}$ L-ascorbic acid 2-phosphate, 10 ng mL^{-1} Transforming Growth Factor—beta 1 (TGF- β 1; R&D Systems, Minneapolis, USA) and 10^{-7} M dexamethasone. To confirm the chondrogenic capacity of the seeded BMSCs, pellet cultures of 250 000 BMSCs/pellet were included as positive controls. Therefore, BMSCs were suspended at a density of 5×10^5 cells mL^{-1} . Aliquots of 0.5 mL cell-suspension were transferred into polypropylene tubes and pellets were formed by centrifuging at 200 G for 8 min.

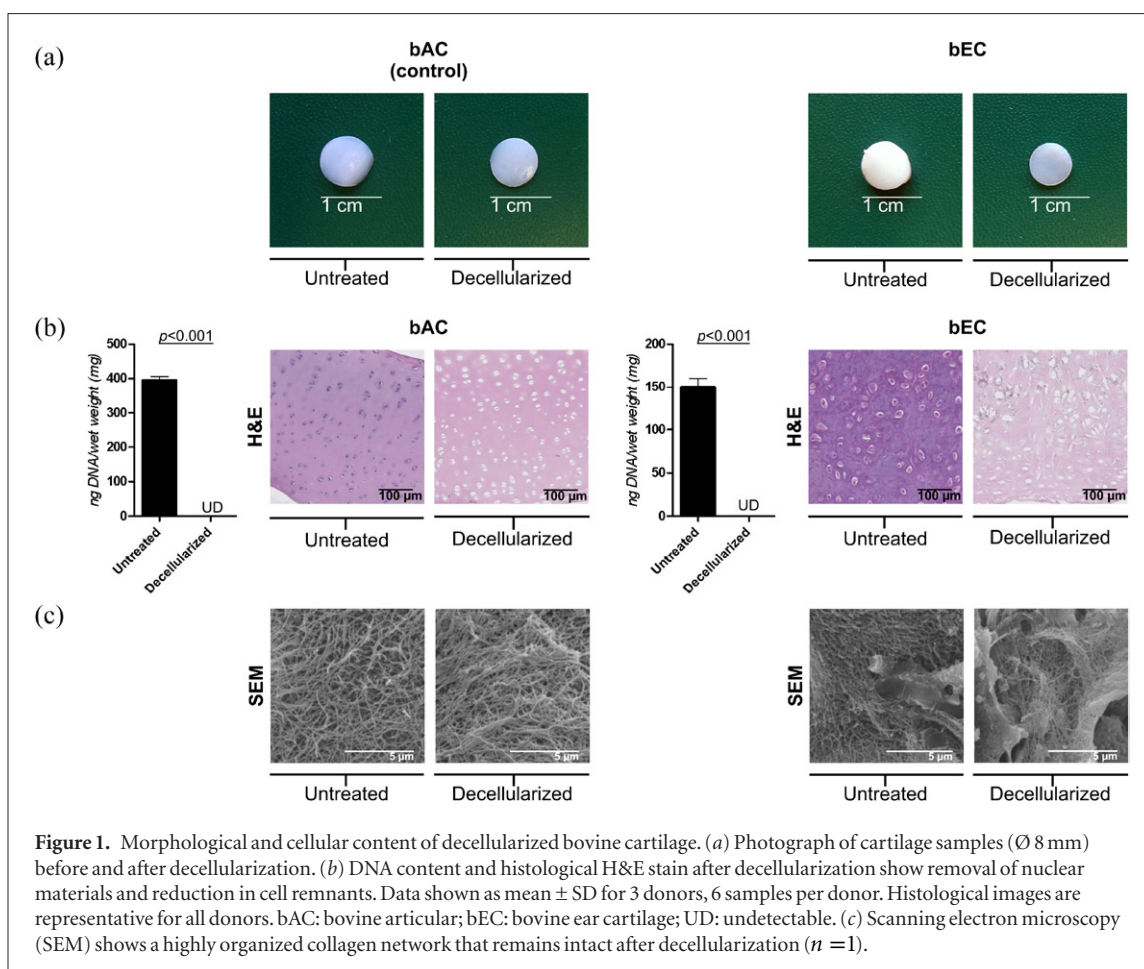
Negative controls included BMSCs cultured in monolayer in DMEM-HG containing 10% FCS, 50 $\mu\text{g}/\text{mL}^{-1}$ gentamicin, 1.5 $\mu\text{g}/\text{mL}^{-1}$ Fungizone and 25 $\mu\text{g}/\text{mL}^{-1}$ L-ascorbic acid 2-phosphate in the absence of TGF- β 1. Samples intended for gene-expression analysis and viability analysis were cultured for 21 d at 37 °C and 5% CO_2 and medium was refreshed twice a week.

After culture, cell viability was evaluated with a LIVE/DEAD® assay (Invitrogen, Carlsbad, USA) according to manufacturer’s instructions. Fluorescent imaging was performed on a Zeiss LSM 510 with the excitation laser set at 488 nm. A 505–530 nm band-pass filter was used to detect living cells and a 650 nm low-pass filter for detecting dead cells.

To assess the chondrogenic differentiation of the BMSCs cultured on the scaffolds, gene expression analysis was performed. RNA was isolated from the seeded scaffolds by snap freezing in liquid nitrogen followed by pulverization using a Mikro-Dismembrator (B. Braun Biotech International GmbH, Melsungen, Germany) at 2800 rpm. The tissue was homogenized with 18 $\mu\text{L}/\text{mg}$ sample RNA-Bee™ (Tel-Test Inc., Friendswood, USA) and 20% chloroform. RNA was isolated using the RNeasy Micro Kit (Qiagen, Hilden, Germany) according to manufacturer’s instructions. Quantification of total extracted RNA was determined using a NanoDrop ND-1000 spectrophotometer (Thermo Fisher Scientific Inc., Waltham, USA) at 260/280 nm. Next, complementary DNA (cDNA) was synthesized using the RevertAid™ First Strand cDNA Synthesis Kit (Fermentas GmbH, Leon-Rot, Germany) according to manufacturer’s instructions. Finally, PCR analysis was accomplished with a Bio-Rad CFX96 Real-Time PCR Detection System using TaqMan® Universal PCR Master Mix (Applied Biosystems) or qPCR™ Mastermix Plus for SYBTR® Green I (Eurogentec). Gene expression of collagen type II (*COL2A1*, Forward: GGCAATAGCAGGTTTCACGTACA; Reverse: CGATAACAGTCTTGC-CCCCTT), SRY (sex determining region Y)-box 9 (*SOX9*, Forward: CAACGCCGAGCTCAGCA; Reverse: TCCACGAAGGGCCGC) and aggrecan (*ACAN*, Forward: TCGAGGACAGCGAGGCC, Reverse: TCGAGGGTGTAGCGTGTAGAGA) was evaluated. Glyceraldehyde-3-phosphate dehydrogenase (*GAPDH*, Forward: ATGGGGAAGGTGAAGGTCG; Reverse: TAAAAGCAGCCCTGGTGACC), Beta-2-Microglobulin (*B2M*, Forward: TGCTCGCGCTACTCTCTCTTT; Reverse: TCTGCTGGATGACGTGAGTAAAC) and hypoxanthine phosphoribosyltransferase 1 (*HPRT1*, Forward: TATGGACAGGACTGAACGTCTTG; Reverse: CACACAGAGGGCTACAATGTG), were used to determine a best-housekeeping-gene-index (BHKi) [35], which was used as reference for the expression of the genes of interest. The relative gene expression was calculated by the $2^{-\Delta CT}$ formula.

2.6. Statistics

The mean and standard deviation (SD) of the variables of interest were calculated using MS Excel 2013 and



PASW Statistics 21.0 (SPSS Inc. Chicago, USA) for 3 independent bovine donors per cartilage type, with 6 samples per donor. For statistical evaluation, a mixed linear model was used followed by a Bonferroni's post-hoc comparisons test. Treatment and cartilage type were defined as fixed factors in the model, while donor was considered as a random factor. Linear regression analysis was performed to evaluate the relationship between amount of matrix components and biomechanical properties after decellularization. For analysis, the mechanical properties (i.e. σ_{\max} , $t_{1/2}$ and E_{eq}) were defined as the dependent variables and matrix components (i.e. GAG, collagen and elastin content) as independent variables. Differences in gene expression of the BMSCs seeded on decellularized cartilage scaffolds were determined by Mann–Whitney U-tests with the genes of interest (i.e. *SOX9*, *COL2A1* and *ACAN*) set as test variables. Differences between human decellularized and untreated cartilage samples for 1 donor in 6-fold, were determined by Mann–Whitney U-tests as well with the biochemical parameters (i.e. DNA, GAG, collagen and elastin contents) as test variable. Differences were considered statistically significant for $p < 0.05$.

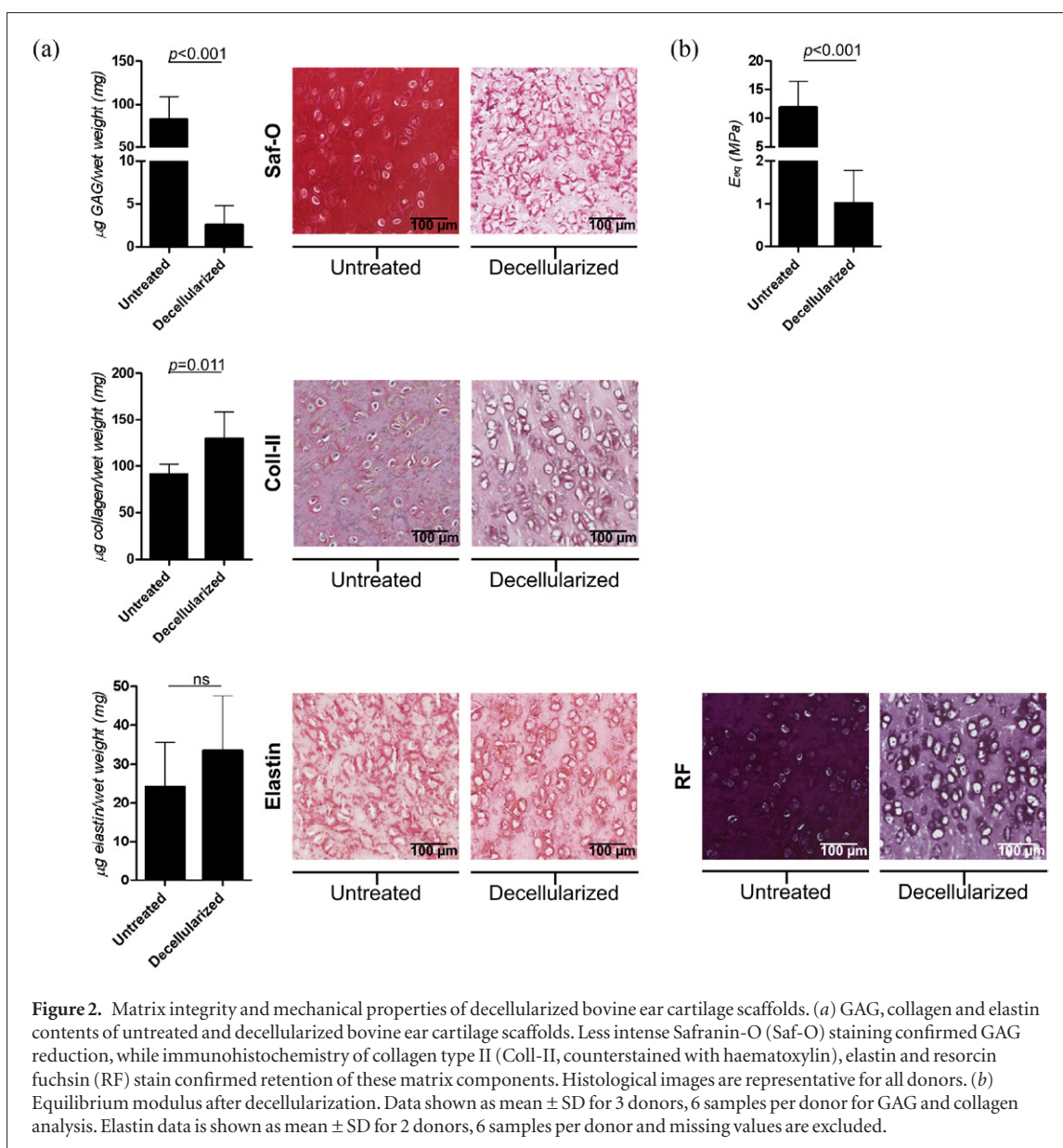
3. Results

3.1. Decellularization of bovine ear cartilage

Bovine cartilage samples were decellularized according to the protocol of Kheir *et al* [19], which was further

optimized to specifically decellularize bEC by the addition of a treatment with a low concentration elastase solution. Bovine articular cartilage (bAC) samples were taken as controls, since AC decellularization has been performed by Kheir *et al* (online supplementary figure 1) (stacks.iop.org/BMM/10/015010). After decellularization, bEC scaffolds and bAC control scaffolds retained their cartilage-like appearance, although samples seemed more translucent after the decellularization process. After decellularization, wet weight reduced by $26.1 \pm 4.9\%$ in bEC and an $8.4 \pm 2.6\%$ wet weight reduction was measured in bAC. The thickness of decellularized bEC scaffolds was significantly reduced ($p < 0.001$) by 23.5% (1.37 ± 0.32 mm) when compared to untreated bEC scaffolds (1.72 ± 0.40 mm), while no obvious reduction in sample diameter was observed (figure 1(a)).

To assess decellularization efficiency, cell content was analyzed histologically (H&E stain) and biochemically. DNA content was significantly reduced ($p < 0.001$) and undetectable (< 10 ng/sample) after decellularization compared to untreated bEC. Similar results were obtained in the decellularized bAC control scaffolds; DNA was significantly reduced ($p < 0.001$) and undetectable after decellularization compared to untreated bAC. Histological analysis showed that the cell remnants were diminished after decellularization and those that were still present were clearly reduced in size and weakly stained for H&E. The ECM itself was weakly



stained compared to the untreated scaffolds, although the overall structure of the ECM was virtually intact (figure 1(b)).

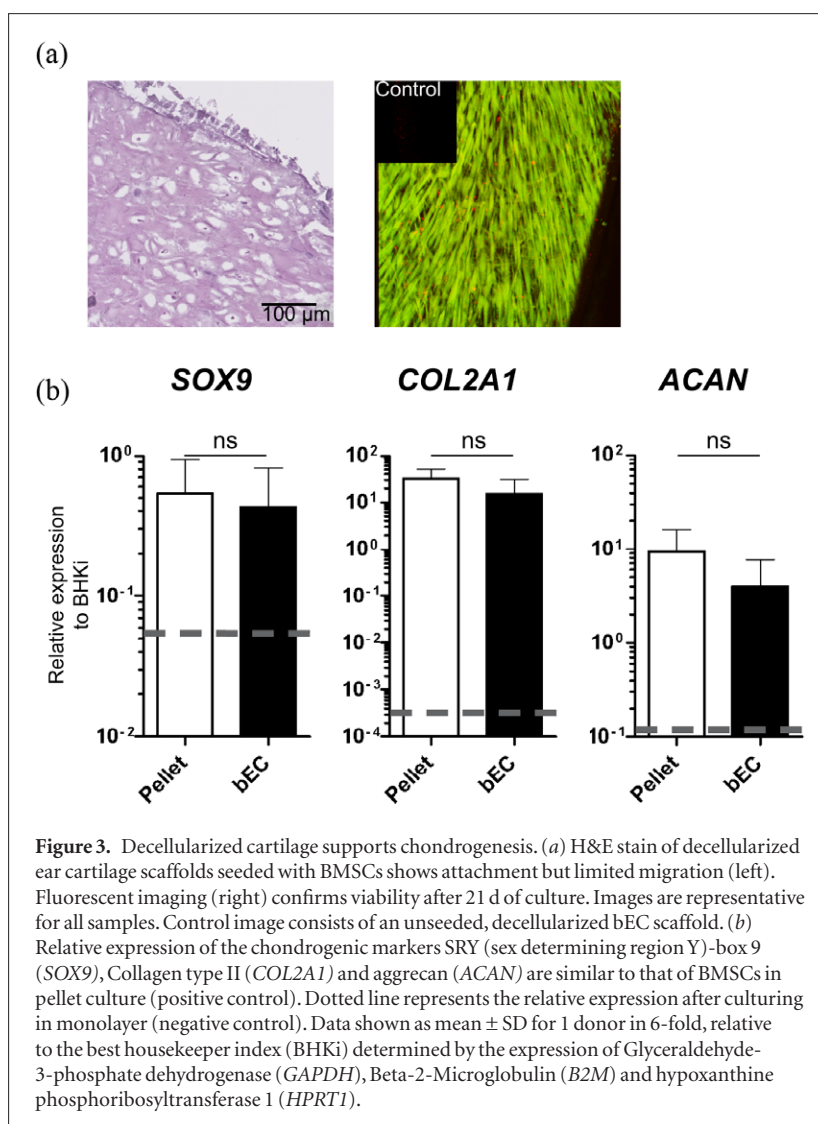
SEM analysis showed no obvious changes in the extracellular matrix after decellularization compared to untreated cartilage. The decellularized bAC and bEC scaffolds retained their dense matrix consistent of fine, intact collagen fibers similar to that of untreated cartilage. In untreated bEC, the thick elastic fibers were deeply embedded and intertwined within a homogeneous collagen network and this 3D organization was retained after decellularization (figure 1(c)).

3.2. Scaffold characterization

To characterize the matrix properties of the decellularized bEC scaffolds, the GAG, total collagen and elastin contents were measured biochemically in addition to histological evaluation. The GAG content of decellularized bEC scaffolds significantly reduced to 3% ($p < 0.001$) compared to untreated bEC, which was confirmed by histological analysis when stained

for Safranin-O. The total collagen content of untreated bEC did not reduce after decellularization, but significantly increased ($p = 0.011$). This phenomenon appears to be due to the normalization of the collagen content to the sample wet weight, since wet weight was reduced after decellularization while the collagen content most likely was not. As GAG content was strongly reduced by the decellularization procedure, the relative contribution of collagens to the overall wet weight increased, resulting in the observed increase in collagen content. Furthermore, immunohistochemical analysis confirmed the retention of collagen type II after decellularization. As for the retention of elastin, no statistical difference was seen between the elastin content of decellularized bEC scaffolds compared to untreated bEC ($p = 0.535$). Histological analysis revealed that after decellularization, elastin was mainly retained directly around lacunae when stained for RF (figure 2(a)).

The biomechanical properties of decellularized cartilage scaffolds were assessed using stress-relaxation-



indentation. A statistically significant reduction of all compressive parameters was seen in decellularized bEC scaffolds compared to the untreated bEC samples ($p < 0.001$). Equilibrium modulus (E_{eq}) of the decellularized bEC scaffolds was 8.7% of the untreated bEC scaffolds. Similarly, maximum stress (σ_{max}) and relaxation half time ($t_{1/2}$) were reduced to 9.2% and 32% of the untreated values, respectively. Specifically, σ_{max} in the decellularized bEC scaffolds was 0.54 ± 0.36 MPa and 5.83 ± 2.18 MPa in untreated bEC. $t_{1/2}$ in the decellularized bEC samples was 0.74 ± 0.45 s compared to untreated 2.31 ± 1.5 s (figure 2(b)). Similar changes in matrix integrity and viscoelasticity were seen in the control group consisting of decellularized bAC scaffolds (online supplementary figure 2)(stacks.iop.org/BMM/10/015010).

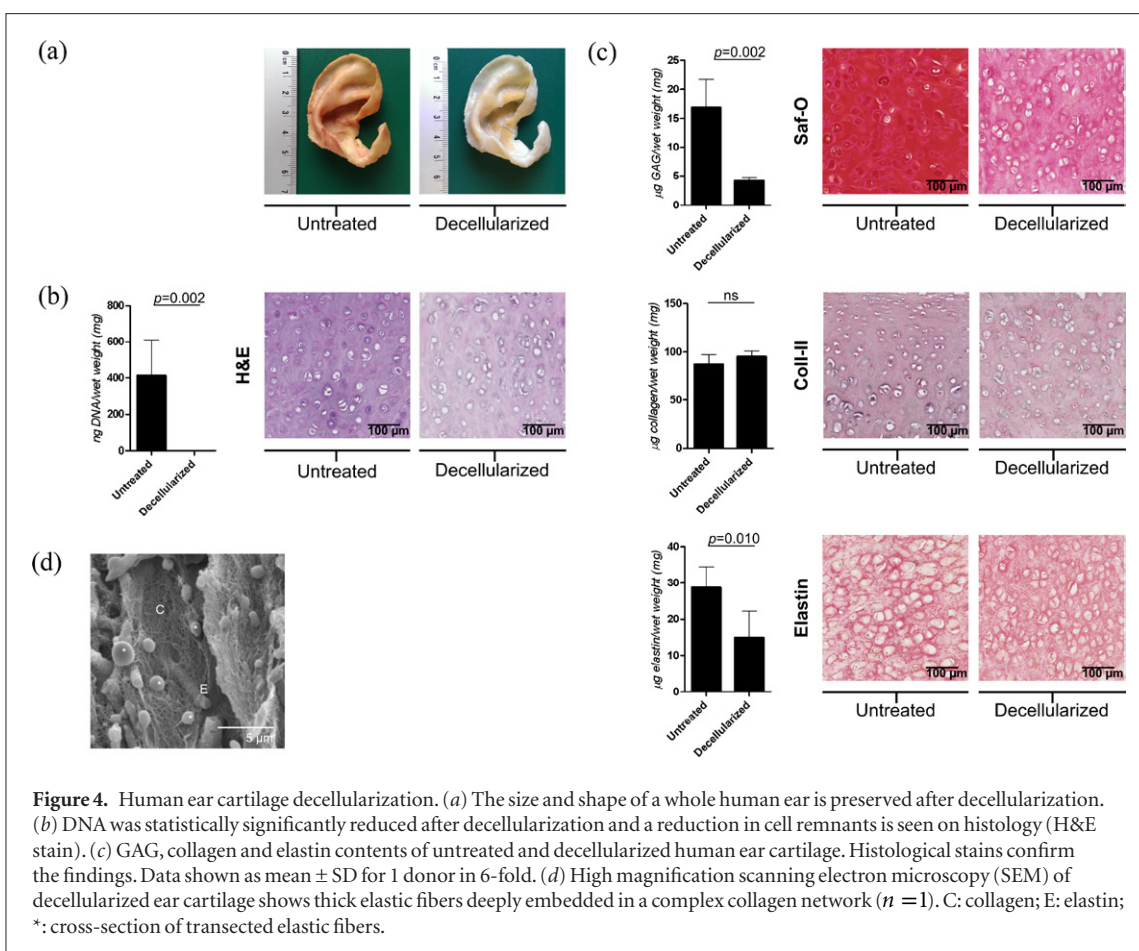
Linear regression analysis was used to correlate ECM components and biomechanical properties. R^2 -values showed that the GAG, collagen and elastin content of the scaffolds were responsible for more than 50% of the biomechanical properties of decellularized cartilage scaffolds: E_{eq} ($R^2 = 0.64$), $t_{1/2}$ ($R^2 = 0.51$) and σ_{max} ($R^2 = 0.618$). GAG content was statistically significantly correlated to E_{eq} ($p = 0.002$), σ_{max} ($p = 0.005$)

and $t_{1/2}$ ($p = 0.001$) of the decellularized bEC and bAC scaffolds.

3.3. Decellularized ear cartilage scaffolds are not cytotoxic and allow chondrogenic differentiation of human BMSCs

To assess the cytocompatibility of the bEC scaffolds, the metabolic activity of plated human BMSCs in the presence of decellularized bEC scaffolds was measured after 4 d of culture. No statistically significant effect on the metabolic activity of the BMSCs due to the decellularized scaffolds was found ($p = 0.559$). Relative to the control wells, $90.76 \pm 8.22\%$ of the cells were viable in the presence of a decellularized bEC scaffold, compared to the conditions in the absence of a scaffold. This indicates that decellularized bEC scaffolds are non-cytotoxic and suitable for cell seeding.

To evaluate survival of human BMSCs in contact with decellularized bEC scaffolds, a LIVE/DEAD® assay was performed after 21 d of culture. Living BMSCs emitted a bright green fluorescence and showed a stretched morphology. Evaluation of z-stacks indicated that the seeded BMSCs were present on the surface of the scaffold. Unseeded, decellularized bEC scaffolds served



as a control and no sign of living cells was observed in these controls. Histological sections showed that after 21 d, BMSCs were attached to the decellularized scaffolds, yet no migration into the scaffolds was observed (figure 3(a)).

Gene-expression analysis of *GAPDH*, *B2M* and *HPRT1* confirmed the presence of BMSCs on decellularized bEC scaffolds after cell-seeding. In decellularized, non-seeded control scaffolds, the expression of either housekeeping gene was non-detectable (CT-values > 40). The chondrogenic potential of BMSCs in pellet culture was confirmed by the expression of the chondrogenic-specific genes *SOX9*, *COL2A1* and *ACAN*, while low expression presented after culturing in monolayer (negative control). Gene expression levels after seeding and culturing on decellularized bEC scaffolds were similar to pellet culture. This shows that decellularized bEC scaffolds support the retention of the chondrogenic capacity of human BMSCs *in vitro* (figure 3(b)).

3.4. Decellularization of human ear cartilage

To investigate the potential clinical implementation of a decellularized scaffold with desirable size and shape, human ear cartilage (hEC) was decellularized and characterized. On gross examination, the size and shape of the whole human ear was preserved after decellularization (figure 4(a)). The DNA content significantly reduced by 99.93% ($p = 0.002$) after decellularization compared to untreated hEC.

Staining for H&E revealed the removal of most nuclear material, with minimal disruption of the ECM structure (figure 4(b)). GAG and elastin contents were significantly reduced in the decellularized hEC scaffolds by 75.3% ($p = 0.002$) and 48.8% ($p = 0.010$), respectively. No statistically significant reduction was seen in the total collagen content ($p = 0.180$) after decellularization and histological staining of the decellularized hEC scaffolds confirmed the biochemical analysis (figure 4(c)). The E_{eq} of the hEC scaffolds was 2.51 ± 1.26 MPa after decellularization and high magnification SEM of the decellularized hEC scaffolds showed a dense collagen matrix intertwined with thick elastic fibers (figure 4(d)).

4. Discussion

For successful cartilage regeneration 3D scaffolds are crucial. We were able to obtain decellularized bovine and human scaffolds from whole full-thickness ear cartilage (EC) tissue. These scaffolds preserved their native collagen and elastin contents, as well as their major architecture and shape. Furthermore, these decellularized EC scaffolds were non-cytotoxic and have the capacity to allow chondrogenic differentiation of human BMSCs *in vitro*.

To date, decellularized scaffolds are extensively used for the reconstruction of various tissues and organs [36]. In addition, several cartilaginous structures have been decellularized. These studies, however, mainly

focus on hyaline (i.e. articular cartilage, nasal cartilage, tracheal cartilage) or fibrous (i.e. meniscal cartilage, annulus fibrosis) cartilaginous tissues. Other cartilage decellularization techniques described in the literature are the fabrication of decellularized ECM-derived scaffolds, by either pulverizing cartilage tissue [29, 30] or stacking thin cartilage slices [37]. Although these seem effective methods to decellularize the tissue, their major drawback is that it completely disrupts the native tissue architecture and/or shape. In fact, no method to specifically decellularize full thickness EC has been described in the literature yet. This study is the first to evaluate structural and functional properties of decellularized full-thickness EC scaffolds of both bovine (bEC) and human (hEC) origin.

Various decellularization protocols are proposed for cartilaginous tissues, each aiming to maximize the decellularization effect, while reducing any adverse effect of the process on the structural composition and functionality of the remaining ECM. Therefore, decellularization outcome was evaluated based on: (1) the removal of cellular material and (2) matrix integrity which was characterized by its components, architecture and biomechanical properties. First, removal of native cellular material is highly imperative, as it reduces the possibility of an immune reaction in case of *in vivo* implantation. For this reason, one of the criteria for successful decellularization is to reduce the DNA content to less than 50 ng/mg tissue [38]. Unfortunately, most recently developed decellularization protocols for cartilage do not meet this requirement at all [18, 25]. These decellularized cartilage scaffolds still show distinct cell remnants on histological examination [12–14, 17–19, 24, 25, 39–42] or need multiple decellularization cycles to remove nuclear material [19, 42], leading to further degradation of the ECM. To specifically decellularize EC, the samples were decellularized according to the protocol of Kheir *et al* [19] which was further optimized to ensure the decellularization outcome was satisfactory for EC and cell remnants reduced. The incorporation of an additional 24 h incubation with a low concentration of elastase (0.03 U/mL) enabled the removal of nuclear material and a reduction of cell remnants in decellularized bEC scaffolds and near-complete removal in decellularized full size human ear cartilage scaffolds. It should be noted though, that the 10 ng detection limit of the DNA assay concerns a fraction of papain digest used in the DNA assay (50 μ l). Because the DNA content was undetectable in that fraction of the decellularized bEC scaffolds, it is reasonable to assume that DNA was removed from the entire scaffolds after decellularization.

Second, the balance between the removal of nuclear material and preserving the matrix integrity should be considered carefully. We showed that the decellularized EC scaffolds preserved their native collagen and elastin contents, as well as their major architecture and shape, while GAG content significantly decreased during the process. Collagen, the most abundant protein present

within the ECM, is of major importance, providing mechanical strength and guiding chondrogenic differentiation [43]. Additionally, the number of collagen cross-links contributes to the mechanical properties of newly formed cartilage [44]. Naturally, we expect these cross-links to be greater in scaffolds derived from native cartilage, than in synthetic scaffolds or ECM-derived scaffolds. Therefore, the retention of collagen during decellularization is crucial. Although collagen type I-elastin-GAG scaffolds were produced before [45], the dense elastic network that is interspersed with the collagen fibrils is not as highly organized as that of native ear cartilage [46, 47], while high magnification SEM showed that the decellularized EC retained the complex interaction between the elastic fibers and fine collagen network. Following decellularization, GAG content decreased significantly which corresponds with previously reported findings by others [18, 19] and was most likely caused by the SDS-treatment during decellularization. Consequently with the GAG reduction, the viscoelastic material properties of the decellularized EC scaffolds also reduced, which is in agreement with findings previously reported by others [48]. Depletion of GAGs might be required to allow cells and cell residuals to leave the matrix [49]. Depending on the eventual application of the scaffold, GAG depletion might also improve ingrowth of cells with chondrogenic capacity into the scaffold and thereby allowing matrix remodeling and revitalization of the graft.

To completely assess functionality of the decellularized scaffold, mechanical properties were evaluated, since it should provide sufficient mechanical strength to compensate for that of the damaged tissue. After decellularization, biomechanical properties reduced significantly. Nevertheless, the decellularized bEC scaffolds presented superior mechanical properties compared to that of other commonly used natural or synthetic biomaterials for cartilage TE. For instance, low equilibrium moduli were found by unconfined compression in various hydrogels; maximum E_{eq} of 0.03 MPa in 2% alginate constructs [50], 0.3 MPa in 20% polyethylene glycol and 0.5 MPa in 15% agarose [51], showing that these hydrogels only reach a maximum of 50% of the E_{eq} of our decellularized EC scaffolds. Additionally, the E_{eq} of synthetic co-polymer scaffolds was 0.05–0.25 MPa [52], which was only 5.5–25% found in our decellularized bEC scaffolds.

To assure long lasting properties and fully functional cartilage, eventual revitalization of the scaffold is a requirement. It is therefore important that we can prepare scaffolds that are non-cytotoxic after decellularization so cells can attach and survive. We showed that our decellularized scaffolds were non-cytotoxic and the seeded BMSCs were still viable after 21 d of culture. Furthermore, the scaffold allowed chondrogenic differentiation of BMSCs. We have used BMSCs in this work to evaluate the cell supportive capacity of our scaffold, the final choice of cell sources would mainly depend on the application and could be any cell with chondrogenic potential such as chondrocytes, perichondrium cells

or adipose derived mesenchymal stem cells [53, 54]. Moreover, it would not be unlikely that seeding prior to implanting a decellularized scaffold is required, as it is the scaffold that could provide support for cells present at the implantation site to grow in. To revitalize and remodel the matrix, migration of cells throughout the matrices needs to be further optimized. In this respect, the reduction of GAGs in the decellularized scaffolds will be advantageous [49], since it has been reported that chondrocyte adhesion is prevented by GAGs [55]. Given that cell adhesion is essential for cell migration, partial or even complete depletion of GAGs could be beneficial to realize cartilage revitalization, as it has been shown that chondrogenic progenitor cells possess the capacity to migrate through degraded cartilage and repair ECM [56]. This indicates that optimization of cell migration could lead to matrix synthesis and restored biomechanical properties of the revitalized cartilage. Recovery of biomechanical properties due to matrix deposited by cells was previously seen by Reiffel *et al* [57], who reported *de novo* cartilage deposition and a 30-fold increase in E_{eq} 3 months after *in vivo* implantation of a collagen type I hydrogel. This showed that the biomechanical properties returned to the native situation.

Finally, the decellularized hEC scaffolds and whole human ear preserved their size and shape after decellularization. Also, approximately 25% more GAGs were retained than in the decellularized bEC. The maturity of the hEC matrix might cause better retention of GAG. In human ears, the ECM components and especially elastic fibers structurally change over the years [46]. When stained for elastin, the elastic fibers in our bEC are mainly directly located as a band around the lacunae whereas in hEC, this network extends more into the ECM, confirming what is shown previously by Ito *et al* [46]. This difference in elastic fibers in adult cartilage, could have protected the ECM from degradation during decellularization. Importantly, this retention was also reflected in the E_{eq} of the hEC scaffolds, which was not reduced compared to that of native hEC (3.3 ± 1.3 MPa for E_{eq}) measured in our previous work [34]. This shows that the decellularization process can also be translated to human tissue and provides the possibility to use decellularized ear cartilage as an improved reconstruction strategy.

5. Conclusion

Decellularization can provide scaffolds made of natural materials, even allogeneic or xenogeneic, for reconstruction of defects in cartilaginous structures. We have prepared decellularized ear cartilage scaffolds with an architecture and matrix composition that closely resembles native cartilage and that have the capacity to support chondrogenic differentiation of BMSCs. Furthermore, the translation of the decellularization method to whole human ear cartilage shows the possibility to use decellularization as an improved reconstruction strategy for large cartilage defects that hold complex shapes. In order to implement the

method as a clinical treatment, long term *in vivo* studies should be conducted to assess the scaffold functionality and characteristics after implantation.

Acknowledgments

The authors would like to thank Professor Dr Gert-Jan Kleinrensink (Department of Neurosciences and Erasmus MC SkillsLab) and Cornelia Schneider (LBI/Red Cross Blood Transfusion Service of Upper Austria) for providing human cartilage. Thanks to Marcel Vermeij (Department of Pathology, Erasmus MC) for his help with the RF stain, Dr Gert-Jan Kremers (Optical Imaging Centre, Erasmus MC) for his help with fluorescent imaging, Professor Dr Heinz Redl (LBI for Experimental and Clinical Traumatology) for his comments on the manuscript. And finally, the authors would like to thank Mairéad Cleary (Department of Orthopaedics, Erasmus MC/University College Dublin) for thoroughly reading the manuscript and providing constructive comments. This study was partially supported by the FFG-Bridge grant CartiScaff (842455).

Conflict of interest

The authors declare that they have no conflict of interest.

References

- [1] Lutolf M P, Gilbert P M and Blau H M 2009 Designing materials to direct stem-cell fate *Nature* **462** 433–41
- [2] Prendergast P J, Huijskes R and Soballe K 1996 ESB Research Award, Biophysical stimuli on cells during tissue differentiation at implant interfaces *J. Biomech.* **30** 539–48
- [3] Huttmacher D W 2000 Scaffolds in tissue engineering bone and cartilage *Biomaterials* **21** 2529–43
- [4] Nayyer L, Birchall M, Seifalian A M and Jell G 2013 Design and development of nanocomposite scaffolds for auricular reconstruction *Nanomed.: Nanotechnol. Biol. Med.* **10** 235–46
- [5] Walser J, Caversaccio M D and Ferguson S J 2013 Electrospinning auricular shaped scaffolds for tissue engineering *Biomed. Tech. (Berl)* **58** (Suppl. 1)
- [6] Romo T, Presti P M and Yalamanchili H R 2006 Medpor alternative for microtia repair *Facial Plast. Surg. Clin. North Am.* **14** 129–36
- [7] Sivayoham E and Woolford T J 2012 Current opinion on auricular reconstruction *Curr. Opin. Otolaryngol. Head Neck Surg.* **20** 287–90
- [8] Bichara D A *et al* 2012 The tissue-engineered auricle: past, present, and future *Tissue Eng. B* **18** 51–61
- [9] Cenzi R, Farina A, Zuccarino L and Carinci F 2005 Clinical outcome of 285 Medpor grafts used for craniofacial reconstruction *J. Craniofacial Surg.* **16** 526–30
- [10] Nayyer L *et al* 2012 Tissue engineering: revolution and challenge in auricular cartilage reconstruction *Plast Reconstr. Surg.* **129** 1123–37
- [11] Badylak S F, Taylor D and Uygun K 2011 Whole-organ tissue engineering: decellularization and recellularization of 3D matrix scaffolds *Annu. Rev. Biomed. Eng.* **13** 27–53
- [12] Ma R *et al* 2013 Structural integrity, ECM components and immunogenicity of decellularized laryngeal scaffold with preserved cartilage *Biomaterials* **34** 1790–8
- [13] Baiguera S *et al* 2010 Tissue engineered human tracheas for *in vivo* implantation *Biomaterials* **31** 8931–8

- [14] Macchiarini P et al 2008 Clinical transplantation of a tissue-engineered airway *Lancet* **372** 2023–30
- [15] Macchiarini P, Walles T, Biancosino C and Mertsching H 2004 First human transplantation of a bioengineered airway tissue *J. Thorac Cardiovasc. Surg.* **128** 638–41
- [16] Laurance J 2010 British boy receives trachea transplant built with his own stem cells *BMJ* **340** c1633
- [17] Elliott M J et al 2012 Stem-cell-based, tissue engineered tracheal replacement in a child: a 2 year follow-up study *Lancet* **380** 994–1000
- [18] Elder B D, Kim D H and Athanasiou K A 2010 Developing an articular cartilage decellularization process toward facet joint cartilage replacement *Neurosurgery* **66** 722–7 discussion 7
- [19] Kheir E, Stapleton T, Shaw D, Jin Z, Fisher J and Ingham E 2011 Development and characterization of an acellular porcine cartilage bone matrix for use in tissue engineering *J. Biomed. Mater. Res. A* **99** 283–94
- [20] Lumpkins S B, Pierre N and McFetridge P S 2008 A mechanical evaluation of three decellularization methods in the design of a xenogenic scaffold for tissue engineering the temporomandibular joint disc *Acta Biomater.* **4** 808–16
- [21] von Rechenberg B et al 2003 Changes in subchondral bone in cartilage resurfacing—an experimental study in sheep using different types of osteochondral grafts *Osteoarthritis Cartilage* **11** 265–77
- [22] Schwarz S et al 2012 Decellularized cartilage matrix as a novel biomatrix for cartilage tissue-engineering applications *Tissue Eng. A* **18** 2195–209
- [23] Elsaesser A F, Bermueller C, Schwarz S, Koerber L, Breiter R and Rotter N 2014 *In vitro* cytotoxicity and *in vivo* effects of a decellularized xenogenic collagen scaffold in nasal cartilage repair *Tissue Eng. A* **20** 1668–78
- [24] Chan L K, Leung V Y, Tam V, Lu W W, Sze K Y and Cheung K M 2013 Decellularized bovine intervertebral disc as a natural scaffold for xenogenic cell studies *Acta Biomater.* **9** 5262–72
- [25] Mercuri J J, Gill S S and Simionescu D T 2011 Novel tissue-derived biomimetic scaffold for regenerating the human nucleus pulposus *J. Biomed. Mater. Res. A* **96** 422–35
- [26] Stapleton T W et al 2008 Development and characterization of an acellular porcine medial meniscus for use in tissue engineering *Tissue Eng. A* **14** 505–18
- [27] Sandmann G H et al 2009 Generation and characterization of a human acellular meniscus scaffold for tissue engineering *J. Biomed. Mater. Res. A* **91** 567–74
- [28] Stabile K J et al 2010 An acellular, allograft-derived meniscus scaffold in an ovine model *Arthroscopy* **26** 936–48
- [29] Kang H et al 2012 *In vivo* cartilage repair using adipose-derived stem cell-loaded decellularized cartilage ECM scaffolds *J. Tissue Eng. Regen. Med.* **8** 442–53
- [30] Yang Q et al 2008 A cartilage ECM-derived 3D porous acellular matrix scaffold for *in vivo* cartilage tissue engineering with PKH26-labeled chondrogenic bone marrow-derived mesenchymal stem cells *Biomaterials* **29** 2378–87
- [31] Farndale R W, Buttle D J and Barrett A J 1986 Improved quantitation and discrimination of sulphated glycosaminoglycans by use of dimethylmethylene blue *Biochim. Biophys. Acta* **883** 173–7
- [32] Creemers L B, Jansen D C, van Veen-Reurings A, van den Bos T and Everts V 1997 Microassay for the assessment of low levels of hydroxyproline *BioTechniques* **22** 656–8
- [33] Stok K S, Lisignoli G, Cristino S, Facchini A and Muller R 2010 Mechano-functional assessment of human mesenchymal stem cells grown in 3D hyaluronan-based scaffolds for cartilage tissue engineering *J. Biomed. Mater. Res. A* **93** 37–45
- [34] Nimeskern L, Martinez Avila H, Sundberg J, Gatenholm P, Muller R and Stok K S 2013 Mechanical evaluation of bacterial nanocellulose as an implant material for ear cartilage replacement *J. Mech. Behavior Biomed. Mater.* **22** 12–21
- [35] Pfaffl M W, Tichopad A, Prgomet C and Neuvians T P 2004 Determination of stable housekeeping genes, differentially regulated target genes and sample integrity: BestKeeper-Excel-based tool using pair-wise correlations *Biotechnol. Lett.* **26** 509–15
- [36] Badylak S F, Weiss D J, Caplan A and Macchiarini P 2012 Engineered whole organs and complex tissues *Lancet* **379** 943–52
- [37] Gong Y Y, Xue J X, Zhang W J, Zhou G D, Liu W and Cao Y 2011 A sandwich model for engineering cartilage with acellular cartilage sheets and chondrocytes *Biomaterials* **32** 2265–73
- [38] Crapo P M, Gilbert T W and Badylak S F 2011 An overview of tissue and whole organ decellularization processes *Biomaterials* **32** 3233–43
- [39] Conconi M T et al 2005 Tracheal matrices, obtained by a detergent-enzymatic method, support *in vitro* the adhesion of chondrocytes and tracheal epithelial cells *Transpl. Int.* **18** 727–34
- [40] Partington L et al 2013 Biochemical changes caused by decellularization may compromise mechanical integrity of tracheal scaffolds *Acta Biomater.* **9** 5251–61
- [41] Remlinger N T et al 2010 Hydrated xenogenic decellularized tracheal matrix as a scaffold for tracheal reconstruction *Biomaterials* **31** 3520–6
- [42] Zang M, Zhang Q, Chang E I, Mathur A B and Yu P 2012 Decellularized tracheal matrix scaffold for tissue engineering *Plast Reconstr Surg.* **130** 532–40
- [43] Chen C W et al 2005 Type I and II collagen regulation of chondrogenic differentiation by mesenchymal progenitor cells *J. Orthop. Res.* **23** 446–53
- [44] Bastiaansen-Jenniskens Y M et al 2008 Contribution of collagen network features to functional properties of engineered cartilage *Osteoarthritis Cartilage* **16** 359–66
- [45] Daamen W F et al 2003 Preparation and evaluation of molecularly-defined collagen-elastin-glycosaminoglycan scaffolds for tissue engineering *Biomaterials* **24** 4001–9
- [46] Ito I, Imada M, Ikeda M, Sueno K, Arikuni T and Kida A 2001 A morphological study of age changes in adult human auricular cartilage with special emphasis on elastic fibers *Laryngoscope* **111** 881–6
- [47] Kostovic-Knezevic L, Bradamante Z and Svajger A 1981 Ultrastructure of elastic cartilage in the rat external ear *Cell Tissue Res.* **218** 149–60
- [48] Mow V C, Ratcliffe A and Poole A R 1992 Cartilage and diarthrodial joints as paradigms for hierarchical materials and structures *Biomaterials* **13** 67–97
- [49] Schwarz S et al 2012 Decellularized cartilage matrix as a novel biomatrix for cartilage tissue-engineering applications *Tissue Eng. A* **18** 2195–209
- [50] Wong M, Siegrist M, Wang X and Hunziker E 2001 Development of mechanically stable alginate/chondrocyte constructs: effects of guluronic acid content and matrix synthesis *J. Orthop. Res.* **19** 493–9
- [51] Roberts J J, Earnshaw A, Ferguson V L and Bryant S J 2011 Comparative study of the viscoelastic mechanical behavior of agarose and poly(ethylene glycol) hydrogels *J. Biomed. Mater. Res. B* **99** 158–69
- [52] Woodfield TB, Malda J, de Wijn J, Peters F, Riesle J and van Blitterswijk CA 2004 Design of porous scaffolds for cartilage tissue engineering using a 3D fiber-deposition technique *Biomaterials* **25** 4149–61
- [53] Pleumeekers M M et al 2014 The *in vitro* and *in vivo* capacity of culture-expanded human cells from several sources encapsulated in alginate to form cartilage *Eur. Cells Mater.* **27** 264–80 discussion 78–80
- [54] Van Osch G J, Mandl E W, Jahr H, Koevoet W, Nolst-Trenite G and Verhaar J A 2004 Considerations on the use of ear chondrocytes as donor chondrocytes for cartilage tissue engineering *Biorheology* **41** 411–21
- [55] Hunziker E B and Kapfinger E 1998 Removal of proteoglycans from the surface of defects in articular cartilage transiently enhances coverage by repair cells *J. Bone Joint Surg. Br.* **80** 144–50
- [56] Koelling S et al 2009 Migratory chondrogenic progenitor cells from repair tissue during the later stages of human osteoarthritis *Cell Stem Cell* **4** 324–35
- [57] Reiffel A J et al 2013 High-fidelity tissue engineering of patient-specific auricles for reconstruction of pediatric microtia and other auricular deformities *Plos One* **8** e56506